Programme nucléon-nucléon à SATURNE II, partie 3, E-225 = Nucleon-Nucleon Program at Saturne II, part 3, E-225

Allgower, Chris E.; Arvieux, J.; Ball, J.; Barabash, L.S.; Bedfer, Y.; Benda, B.; Beddo, M.; Borisov, N.S.; Boutefnouchet, A.; Bystricky, J.; Chamouard, P.-A.; Chaumette, P.; Combet, M.; Demierre, Philippe [**and 37 more**]

Programme Nucléon-Nucléon à SATURNE II, Partie 3, E-225

C.E. Allgower[1], J. Arvieux[2], J. Ball[2], L.S. Barabash[3], Y. Bedfer[2] B. Benda[4], M. Beddo[1], N.S. Borisov[3], A. Boutefnouchet[5], J. Bystricky[4], P.-A. Chamouard[2], P. Chaumette[4], M. Combet[2], Ph. Demierre[6], J. Derégel[4], G. Durand[4], A.P. Dzyubak[4,7], J.-M. Fontaine[2], G. Gaillard[6], C. Gaudron[4], V. Ghazikhanian[5], J.-P. Godour[8], D.P. Grosnick[1], R. Hess[6,†], Z. Janout[3,9], Z.F. Janout[6,10], T.E. Kasprzyk[1], V.A. Kalinnikov[3], Yu.M. Kazarinov[3,†], B.A. Khachaturov[3], R. Kunne[2], F. Lehar[4], A. de Lesquen[4], D. Lopiano[1], M. de Mali[4,†], V.N. Matafonov[3], G. Milleret[2], F. Perrot-Kunne[4], I.L. Pisarev[3], A.A. Popov[3], A.N. Prokofiev[11], D. Rapin[6], L. van Rossum[4], J.L. Sans[2], H.M. Spinka[1], A. Teglia[6], Yu.A. Usov[3], V.V. Vikhrov[11], B. Vuaridel[6], C.A. Whitten[5] and A.A.Zhdanov[11]

1) ANL-HEP, 9700 South Cass Ave., Argonne, IL 60439, USA
2) Laboratoire National SATURNE, CNRS/IN2P3 et CEA/DSM CE-Saclay, 91191 Gif-sur-Yvette Cedex, France
3) LNP-JINR, 141980 Dubna, Moscow Region, Russia
4) CEA-DAPNIA, CE Saclay, 91191 Gif sur Yvette Cedex, France
5) UCLA, 405 Hilgard Ave., Los Angeles, CA 90024, USA
6) DPNC, Université de Genève, 24, quai Ernest-Ansermet, 1211 Geneva 4, Suisse
7) Kharkov Institute of Physics and Technology, Academicheskaya str. 1, 310108 Kharkov, Ukraine,
8) C.E.N.B., Domaine du Haut-Vigneau, 33170 Gradignan, France
9) Faculty of Nuclear Sciences and Physical Engineering, Czech Technical University, Břehová 7, 11519 Prague 1, Czech Republic
10) Computing Center of the Czech Technical University, Zikova 4, 16635 Prague 6, Czech Republic
11) Petersburg Nuclear Physics Institute, 188350, Gatchina, Russia,
†) Deceased

Résumé

Ce rapport contient les résultats obtenus pendant la période 1992 - 1995 dans le cadre du programme Nucléon-Nucléon (NN) auprès de Saturne II. La diffusion *pp* élastique et quasiélasique a été étudiée en détail au-dessus de 1.8 GeV dans un large domaine angulaire. Les mesures ont été effectuées avec les faisceaux de protons polarisés et non-polarisés et/ou avec la cible polarisée. Les observables dépendant des spins des particules initiales ainsi que la polarisation des particules de recul ont été mesurées pour différentes orientations des spins. Les particularités intéressantes et les structures observées dans les dépendances angulaires et en énergie des observables et des amplitudes de diffusion sont présentées.

Nucleon-Nucleon Program at Saturne II - Part 3 : E-225

Abstract

This report contains results obtained during the period 1992 - 1995 in the Nucleon-Nucleon (NN) program at Saturne II. The *pp* elastic and quasielastic scattering has been studied in detail above 1.8 GeV in the large angular range. The measurements were performed with a polarized and unpolarized proton beams and/or with the polarized proton target. Observables depending of the initial particle spins as well as the recoil particle polarizations were measured for different spin direction combinations. Interesting features and structures observed in the energy and angular dependence of the observables and of the scattering amplitudes are discussed.

1. Introduction

During the period 1981-1986 in the NN program (Part 1) the *pp* spin-dependent scattering observables and the total cross section differences were measured. The proton polarized beam and/or the proton polarized target (PPT) [1] were used. About 3000 experimental data points for 13-15 independent observables have been obtained. These data together with known total and differential cross sections allowed to carried out the unambigous *pp* phase shift analyses (PSA) at fixed energies up to 1.80 GeV [2]. Recently, the energy dependent PSA was extendend up to 2.55 GeV [3]. Using the NN data, the complete sets of *pp* observables at Saturne II were determined at 11 energies and several angles from 0.834 to 2.696 GeV [4]. In addition to *pp* elastic scattering, quasielastic *pp* and *np* observables were measured with polarized deuteron beam.

From 1986 to 1990 the NN program (Part 2) continued by similar measurements of the *np* elastic scattering observables with a polarized beam of free neutrons and a new large PPT [5]. The apparatus was completed by a large neutron counter hodoscope provided by the Geneva University. Due to the MIMAS booster, the neutron beam intensity increased to about 10^7 neutron/spill. About 2000 data points were measured and allowed the first direct reconstruction of the *np* scattering amplitudes at 6 energies. Any *np* PSA above 0.8 GeV is based on the Saturne II data [6].

Since 1.1 GeV is close to the maximal neutron beam energy at Saturne II, an extension was only possible using quasielastic scattering of accelerated protons on the polarized deuteron target (PDT). The polarized ^6LiD target was developped and studied [5] by the collaboration of the Saclay, Dubna, ANL, Prague and Kharkov experts. An important part of the target materials (^6LiD and ^6LiH) was provided by the Dubna participants. The *pp* results with ^6LiH are presented here. The OFF-LINE analysis of the recorded quasielastic data will be finished in 1998.

The interesting features and structures obtained in the *pp* data (Part 1) were cross-checked (Part 3) until April 1995. A second superconducting beam solenoid was installed by the target group to obtain a pure sideways proton beam polarization. It could be tuned using a new polarimeter, constructed by the Gatchina physicists. The Saclay MWPC's were considerably improved and operated by the Dubna collaborators. Apparatus was completed by the Argonne MWPC and electronics.

Several anomalies were observed in the beam polarization (P_B) behaviour. Although its value was improved, it remained uncertain if the two opposite proton beam polarizations were strictly equal and if the "unpolarized" beam from the polarized ion source Hyperion was really unpolarized. This was solved by dedicated measurements in 1996 [7].

The apparatus and the PPT (PDT) developments, were presented in earlier issues of "Nouvelles de Saturne". References are reduced to a necessary minimum. An exhaustive list is given in [8]. Mostly the Saturne data are plotted in Figures. The experimental results discussed here were proceeded by the Saclay and Dubna physicists as well as by the ANL participants in two separate OFF-LINE analyses. Results of a common analysis will be published soon. The data presented below are already very close to final results.

2. Determination of Observables

The subscripts of any observable X_{oqij} refer to the polarization states of the scattered, recoil, beam, and target particles, respectively. For the so-called "pure experiments," the polarizations of the incident and target particles in the laboratory system are oriented along the basic unit vectors $\vec{k}$, $\vec{n}$ and $\vec{s} = [\vec{n} \times \vec{k}]$. The recoil protons are analyzed in the directions $\vec{k}$", $\vec{n}$ and $\vec{s}$"$= [\vec{n} \times \vec{k}$"] where the unit vector $\vec{k}$" is oriented along the direction of the recoil particle momentum [9].

The most general formula for the correlated nucleon-nucleon scattering cross section Σ [11] assumes that both initial particles are polarized and that the polarization of scattered and recoil particles are analyzed. The formula does not change whether the fundamental conservation laws are applied or not. It is valid in any reference frame. Here we give the simplified formula valid for the polarized beam and target and for the analyzed recoil particle labeled "2".

$$\Sigma(P_B,P_T,P_2) = I_2(\frac{d\sigma}{d\Omega})_0\Big((1 + A_{oooio}P_{Bi} + A_{oooj}P_{Tj} + A_{ooij}P_{Bi}P_{Tj}) + P_2(P_{oqoo} + K_{oqio}P_{Bi} + D_{oqoj}P_{Tj} + +N_{oqij}P_{Bi}P_{Tj})n_{2q}\Big). \quad (2.1)$$

The summation is implicit over the indices o,q,i,j. Indices i,j correspond to the three basis vectors, index q refers to the unit vectors of Eq.(2.2), index "o" denotes zero. $(d\sigma/d\Omega)_0$ is the differential cross section for single scattering of unpolarized incident and target particles. P_{Bi} and P_{Tj} are the beam and target polarization components, respectively. I_2 and P_2 denote the cross section and the analyzing power for the recoil particle analyzer "2", respectively. If there is no rescattering ($q = o$), we obtain the single scattering observables and $I_2 = 1$ and $P_2 = 0$. The unit vector $\vec{n}_2 = [\vec{k}" \times \vec{k}_r]$ is along the direction of the normal to the recoil particle analyzing plane. Here $\vec{k}_r$ is a unit vector in the direction of the rescattered particle. The scalar product $(\vec{n},\vec{n}_2)$ determines the components n_{2q} for different directions of $\vec{n}_2$.

Observables are related to bilinear combinations of the real and imaginary parts of the scattering amplitudes. We use the invariant amplitudes a,b,c,d and e from Ref.[9].

3. Features of the Analyzing Power

If the beam polarization $\vec{P}_B$ and the target polarization $\vec{P}_T$ are oriented along the vertical axis ($\vec{n}$ perpendicular to the scattering plane), an elastic single scattering experiment provides three observables : A_{oono}, A_{ooon} and A_{oonn}.

The observables A_{oono} and A_{ooon} are equal due to Pauli principle . Counting rates for opposite beam and target spin orientations in the single scattering provide four equations. The asymmetry ratios determine three spin observables A_{oono}, A_{ooon}, and A_{oonn} if P_B and P_T are known. The unpolarized differential cross section in the asymmetry ratios cancels out. If P_B (P_T) is unknown, we can solve the four relations (2.1) for P_B (or P_T), $A_{oono} = A_{ooon}$ and A_{oonn}. Consequently, at a given energy, one can relate P_B to P_T, or vice versa.

The *pp* elastic analyzing power is an antisymmetric function of the CM scattering angle with respect to 90° and is identically equal to zero at 0°, $90°CM$, and $180°CM$. An interesting behavior was observed in the t-dependence of the *pp* analyzing power over a very broad energy domain [10]. Let us consider this observable between 0° and 90° CM where $A_{oono} = A_{ooon}$ crosses zero. At small $-t$ values A_{oono} reaches a first maximum. For $-t \leq 1.0$ $(GeV/c)^2$ the maximal value of A_{oono} decreases monotonically starting from 0.8 GeV.

A minimum at $-t \sim 1.0$ $(GeV/c)^2$ is observed in a large energy region. The A_{oono} values in the minimum may be positive or negative. The negative values were found at SATURNE II from 1.3 to 1.8 GeV [11].

The first minimum is followed by a second maximum around $-t \sim 1.7$ $(GeV/c)^2$ at all energies above 1.1 GeV. Only positive $A_{oono}(pp)$ values are observed at the second maximum. The next minimum appears out of the Saturne energy range at $-t \sim 3.5$ $(GeV/c)^2$.

This is one of the basic structures in the *pp* elastic scattering, first observed at Saturne II. Only the positions of the two minima and of the second maximum are fixed. The magnitude of $A_{oono} = A_{ooon}$ at these three extrema cannot be predicted, extrapolated, or even interpolated over a large energy range. This is in contrast with the first maximum at small angles.

The best fit to the data as a function of energy is that which uses a fixed $-t$ value. In this case the fitted experimental points at all energies are in the same region with respect to the neighbouring extrema.

4. Analyzing Power Data and Beam Polarizations

The apparatus used the NN program is described in Ref. [12]. Recoil protons were always rescattered in the carbon analyzer. The data at each energy were analyzed by the existing standard method [12], using the Alain de Lesquen's program.

At angles above $58°CM$ NN results obtained from 1992 to 1995 were measured at 29 different energies between 1.80 and 2.80 GeV. The data at several energies were remeasured. Altogether 40 different angular distributions, giving about 800 data points for $A_{oono} = A_{ooon}$, were measured. The same amount of data was obtained for spin correlation A_{oonn}. Most of these data used the four Hyperion polarization states, one part was measured with three states, and another part with two states only. All states were used in the first OFF-LINE data analyses and strong fluctuations of the analyzing power energy and angular dependences were observed. These anomalies suggested either a nonzero polarization of at least one "unpolarized" state, or a discrepancy of the magnitude of the two polarized states.

Other factors, as stability of MWPC's, of monitors, and the A_{oono} (A_{ooon}) zero crossing points at $90°CM$, might be also checked. For such checks the best was to perform accurate measurements at 0.80 GeV. At this energy the *pp* analyzing power is well known, having been measured, for example, at SATURNE II, at SATURNE I, at LAMPF, at CERN, at Gatchina, at the BNL Cosmotron, and at ANL-ZGS.

The four polarization beam states and also an unpolarized target were used. The data analysis confirmed a suspicion concerning the beam polarizations from Hyperion. The data suggested new measurements using also a strictly unpolarized proton beam. The results of this dedicated experiment, described in Ref. [7], showed that in the working conditions the opposite polarized Hyperion states provide the same absolute beam polarization values, whereas the "unpolarized" states give $|P_B|$ of about 0.06. The old NN data remain unaffected by this fact, since they were obtained using the polarized states only, but was taken into account in new OFF-LINE analyses.

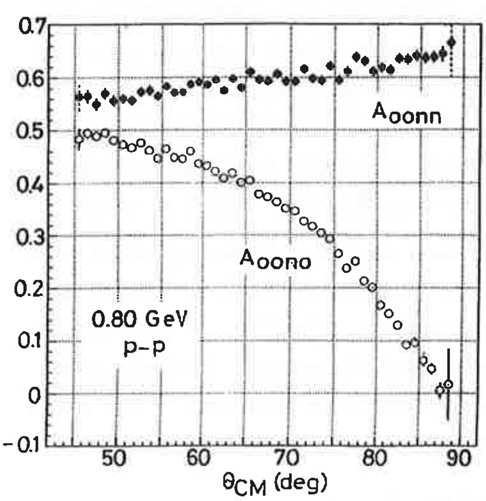

Fig. 1

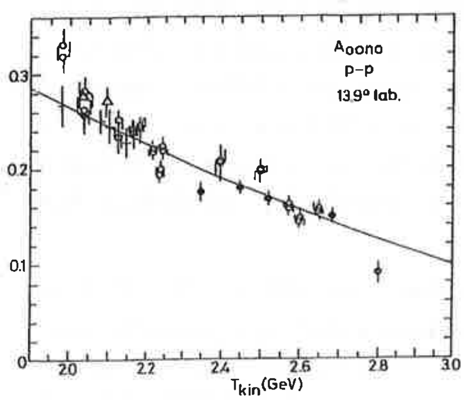

Fig. 2

The results at 0.80 GeV are shown in Fig. 1. The P_B value determined by the NN beam polarimeter was fixed and the P_T value was varied, until fits to A_{oono} and to A_{ooon} coincided. This search is very sensitive to the P_T value.

At high energies, above 1.80 GeV, the procedure was inverted: the P_T value was kept fixed and the P_B value was varied. This was done for the majority of the energies, without taking the polarimeter data into account.

The P_B values were applied to the polarimeter asymmetry data and the analyzing power values for the CH_2 target were obtained. Using the known ratio of the *pp* and CH_2 analyzing power for the NN beam polarimeter at $13.9°$ *lab.*, the energy dependence at this angle was calculated (see Fig. 2). The fit to the data checks the compatibility of the beam polarization, determined by two different methods. The fit to the data at the forward angle represents also updated results for any beam polarimeter.

The A_{oono} energy dependence at large angles is a monotonically increasing function up to 2.70 GeV. Then we observe a decrease at 2.8 GeV. This is shown in Fig. 3 where the energy dependence at $26°$ *lab* is plotted.

Black dots are the new NN data, open circles are from [11], the solid line is our fit, the dashed line is from the PSA [3] without our data. For this reason a disagreement occurs above 2.2 GeV.

The A_{ooon} data recently published in Ref.[13] (133 data points) were measured below 52°CM at 2.16, 2.18, 2.20, 2.22, 2.24, 2.26, and 2.28 GeV (Fig. 4, black dots). They were obtained with an unpolarized beam and with the PPT in order to study the region close to the depolarizing resonance $\gamma G = 6$ at 2.202 GeV. The unpolarized

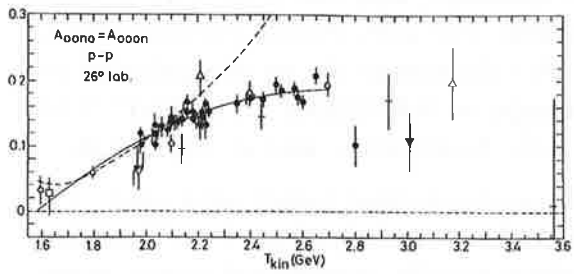

Fig. 3 - Analyzing power at 26°*lab*.

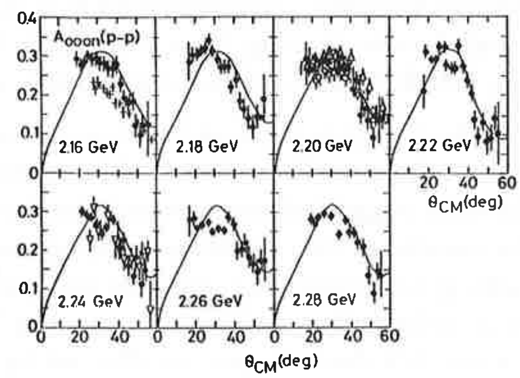

Fig. 4 - A_{ooon} at small angles. Solid lines are predictions of [3], • are NN data.

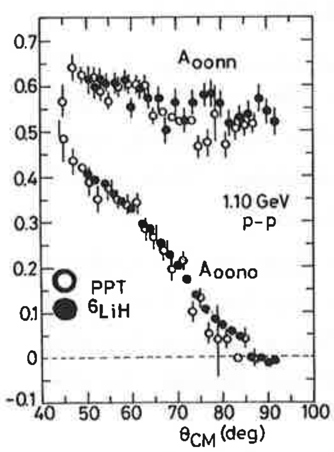

Fig. 5

beam was obtained from Hyperion in state "1" working at nominal conditions, but the correctors for depolarizing resonances were switched off. Moreover, the Hyperion solenoid [7], which rotates low energy particle spins to the vertical direction, was not working. The asymmetry measured with an additional unpolarized target showed the mean absolute value of the unpolarized beam was 0.002 ± 0.004 at most.

Measurements of quasielasic and elastic scattering with the polarized proton beam and the polarized ^6LiD or ^6LiH targets provided mainly *pp* observables. In Fig. 5 are shown the A_{oono} and A_{oonn} angular distributions at 1.10 GeV, measured with ^6LiH and compared with the pentanol PPT data [11,14]. We observe no difference of the results.

5. Spin Correlation Parameter A_{oonn}

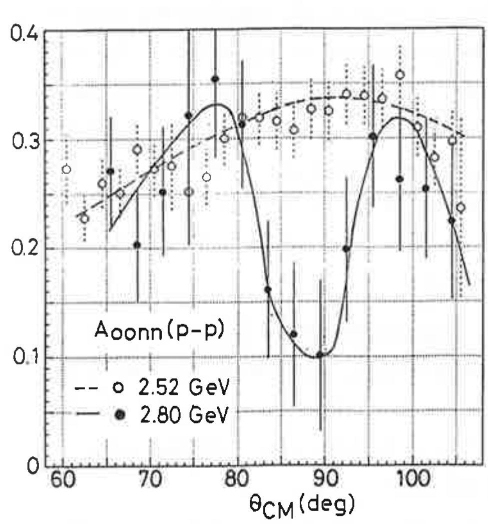

Fig. 6

The single scattering experiment with the polarized beam and target for P_{Bn} and P_{Tn} (Eq.(2.1)) measures also the spin correlation parameter A_{oonn}. The results at 0.80 GeV, also plotted in Fig. 1, are very accurate and are in excellent agreement with the previously published data [14].

In the angular region from 58° to 90° CM the slope of this observable slowly decreases between 1.80 and 2.65 GeV. At 2.80 GeV appears a well pronounced minimum around 90° CM. The observed difference in the angular dependence is shown in Fig. 6 where are plotted the data at 2.52 GeV and at 2.80 GeV. At 2.80 GeV the A_{oonn} value at 90° CM is by a factor 3 smaller than the value at 2.70 GeV. The spin correlation data at this angle above 2.80 GeV was measured at the ANL-ZGS. It remained at a constant of ~ 0.10 up to 4.5 GeV.

6. Depolarization and Polarization Transfer Observables

The rescattering observables were simultaneously measured with single scattering. Recoil particles were rescattered in the carbon analyzer and the Left-Right (L-R) and Down-Up (D-U) asymmetries in the second scattering were measured. The carbon analyzing power was interpolated over the existing data. Using Eq.(2.1) for $\vec{P}_B$ and $\vec{P}_T$ oriented along $\vec{n}$, the analyzing scattering gives P_{onoo}, D_{onon}, K_{onno} and N_{onnn} from the L-R asymmetry. The D-U asymmetry checked an absence of others beam and target polarization components.

K_{onno} at the angle θ_{CM} is equal to D_{onon} at the angle $180° - \theta_{CM}$. $P_{onoo} = N_{onnn}$ are equal to the single scattering quantities A_{oono} and A_{ooon}, which are known with better accuracy. The total of 190 D_{onon} and K_{onno} data points was measured at 28 energies in the angular region from 60° to 110° CM.

7. Spin Correlation A_{oosk} and Other Rescattering Observables

Most of the *pp* amplitude determinations, based on previously measured data at 11 energies between 0.8 and 2.7 GeV, have resulted in a unique type of solution [4]. However two solutions were obtained at 2.1 GeV. One of them is similar to the solutions found at other energies. The second one, more probable, is different and indicates the existence of a possible resonance in a spin-triplet amplitude in the vicinity of this energy. In contrast, the solution with the lower probability did not suggest a spin-triplet resonance for isospin I=1. In order to compare the two solutions at 2.1 GeV, all measurable quantities were calculated using both sets of amplitudes. The predictions differed most for the observables $K_{os''so}$ and N_{onsk}. $K_{os''so}$ was determined in the original data with insufficient accuracy, while N_{onsk} was measured as a linear combination with other observables [2]. A comparison of the predictions with new experimental results could rule out one of the solutions. Measurements of these two observables were performed at 1.80 and 2.10 GeV. The quantities A_{oosk}, D_{onon}, K_{onno}, $D_{os''ok}$, and $N_{os''sn}$ were obtained as by-products. At 1.85 and 2.04 GeV D_{onon} and K_{onno} were also measured.

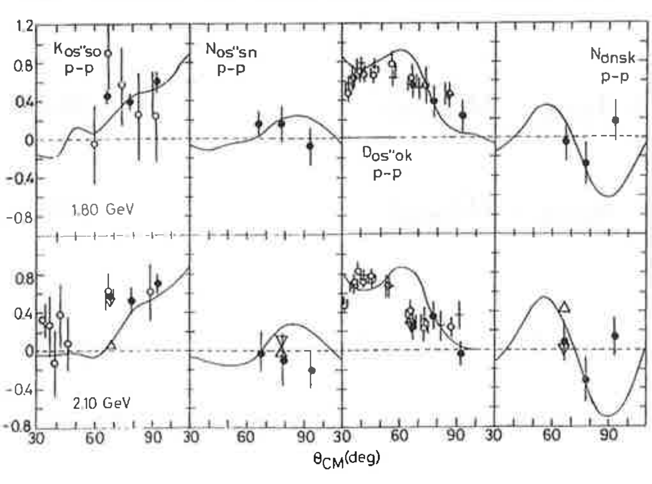

Fig. 7 - Rescattering data. Solid lines - PSA [3], ● - [13], ▽ - the non-resonant solution and △ - the resonant one [4].

Using Eq.(2.1) for P_{Bs} and P_{Tk} we obtain A_{oosk} from the single scattering. From the D-U asymmetry in the second scattering we obtain $K_{os''so}$ and $D_{os''ok}$. The L-R second scattering asymmetry gives P_{onoo} and N_{onsk}.

For P_{Bs} and P_{Tn} single scattering gives A_{ooon} and the second scattering provides $K_{os''so}$ and $N_{os''sn}$.

The initial spin combination P_{Bn} and P_{Tn} was discussed in the Sections 5 and 6. Measurements provided the observables K_{onno} and D_{onon}.

The observables $K_{os"so}$ and D_{onon} were each measured in the two different beam and target spin configurations. This increased statistics and checked an internal compatibily of measurements. All together 40 A_{oosk} and 48 rescattering observables data points were determined [15]. In Fig. 7 are shown the data for four rescattering observables (black dots), compared with former Saturne data and with the PSA predictions [3] without our data. They are compared with two amplitude analysis solutions at 2.10 GeV. We observe an excellent agreement of observables $K_{os"so}$ and N_{onsk} with the non-resonant solution at this energy ($\bigtriangledown$)..

8. Search for Structures

The spin correlation A_{oonn} in pp elastic scattering measured at Saturne II allows to search for a possible structures in the scattering amplitudes. At 2.0 GeV proton beam energy Lomon, LaFrance and Gonzales predicted the existence of a dibaryonic resonance in the $^1S_0$ partial wave (mass 2.7 GeV) (see [16]). Previous data were measured at energies which were too widely separated to determine a narrow structure. Those authors pointed out that the predicted spin-singlet structure, as well as another one near T_{kin} = 2.5 GeV, is suggested by the ANL-ZGS total cross section difference $\Delta\sigma_L(np)$ data. The energy dependence of the pp unpolarized total cross section exhibits no pronounced structure. Indications of anomalies in this energy region were observed in the ANL-ZGS analyzing power measurements. Additional evidence was also suggested by the measurement of the analyzing power A_{yo} in the inelastic channel $pp \to d\pi^+$ and by measurements of the analyzing power and the differential cross section energy dependence in the same reaction (see [17]).

In pp elastic scattering at $90°CM$ three scattering amplitudes survive; a = 0 and b = −c. From the measured A_{oonn} observable and known pp elastic differential cross section $d\sigma/d\Omega$ we can determine the absolute values of the spin-singlet amplitude at $90°CM$:

$$|b|^2 = |c|^2 = \frac{1}{2}\frac{d\sigma}{d\Omega}(1 - A_{oonn}). \qquad (8.1)$$

The remaining two non-zero amplitudes "d" and "e" are pure spin-triplets. In order to determine their absolute values at the same angle, we need an additional knowledge of the observable D_{onon}. It holds :

$$|d|^2 = \frac{1}{2}\frac{d\sigma}{d\Omega}(1 + A_{oonn} - 2D_{onon}), \qquad (8.2)$$

$$|e|^2 = \frac{1}{2}\frac{d\sigma}{d\Omega}(1 + A_{oonn} + 2D_{onon}). \qquad (8.3)$$

At any angle the sum of

$$|a|^2 + |d|^2 + |e|^2 = d\sigma/d\Omega(1 + A_{oonn}) \qquad (8.4)$$

is again pure spin triplet (a(90° CM) = 0), where the errors are given by the well determined A_{oonn} data.

From Eq.(8.1) it follows that a fast decrease of the single scattering observable $A_{oonn}(90°)$ in a small energy range would represent evidence for this structure. In Fig. 8 are plotted $A_{oonn}(90°)$ data measured by the NN group. In figures symbols denote different years of measurements. We observe a large maximum around 1.90 GeV followed by a fast decrease up to 2.24 GeV, constant values up to 2.7 GeV and a very fast decrease at 2.8 GeV. As mentionned in Section 5, the $A_{oonn}(90°)$ values, measured at ANL-ZGS, remain small and constant up to 4.5 GeV at the level of 0.1.

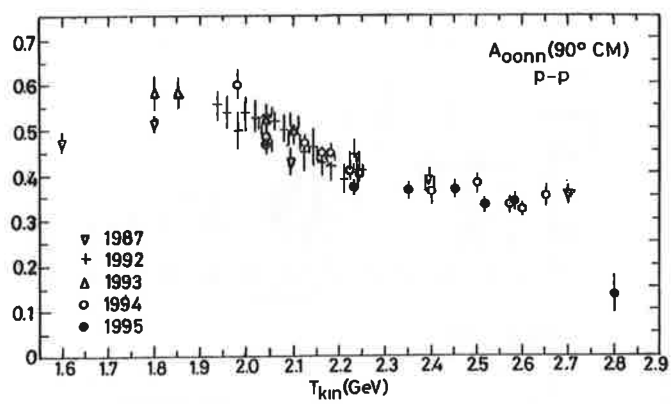

Fig. 8

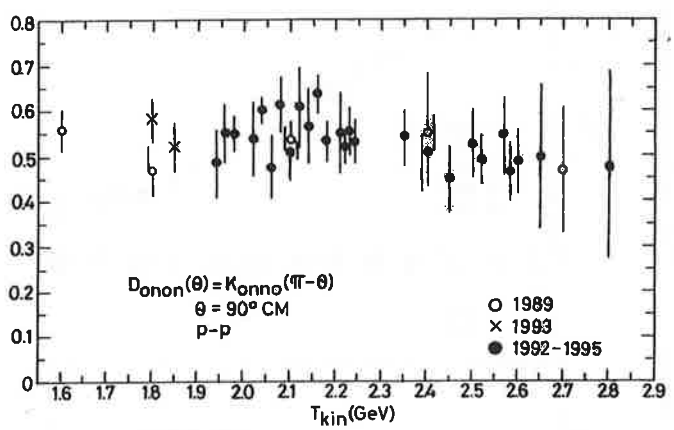

Fig. 9

Fig. 9 shows the energy dependence of D_{onon}. For our purpose the measured values of $D_{onon}(\theta)$ and $D_{onon}(180° - \theta) = K_{onno}(\theta)$ were integrated over 60° to 120° CM angular region. This was possible due to a practically mirror symmetry of the data with respect to 90° CM and a stability of this average value was checked by increase of the integral limits. We observe a constant value within the errors over the whole energy interval.

To obtain the absolute values of the amplitudes we used the *pp* elastic scattering differential cross section from Ref.[18]. This ANL-ZGS experiment covers a very large energy region. The recent PSA [3], using all existing data, is valid below 2.55 GeV only. Results from the PSA [3] and Ref.[18] differ by a normalizing factor of about 35%, which is irrelevant with respect to amplitude energy shapes.

The energy dependence of the absolute values of the three amplitudes at 90° is plotted in Figs. 10, 11 and 12. The $|b|^2 = |c|^2$ shows a well pronounced shoulder centered around 2.1 GeV beam kinetic energy with a width $\Delta T_{kin} = \pm 0.1$ GeV (i.e 2.73 ± 0.04 GeV CM energy). This is in a good agreement with our preliminary results [19]. We also observe a narrow maximum at $T_{kin} = 2.8$ GeV (2.96 GeV CM energy). Above this point the A_{oonn} value drops down with energy as the differerential cross section, due to the constant value from the existing ANL-ZGS results.

The amplitude $|d|^2$, determined with relatively large errors, is a decreasing function of energy from 1.9 to 2.3 GeV. Between 2.4 and 2.6 GeV we observe constant values. The dominant amplitude $|e|^2$ is decreasing in the entire energy interval and is smooth, 2.8 GeV included. The errors of separate amplitudes are related with the errors of D_{onon}. Using Eq.(8.4) we obtain decreasing function with small errors. This is shown for 90° CM in Fig. 13 and for 70° CM in Fig. 14. The errors are within sizes of plotted data points.

Nucleon-nucleon exotic states given in [16] indicate spin-triplet resonance masses higher than the masses for the first two spin-singlet states. It is not surprizing that we observe no indication for a possible resonance in the spin-triplet states. It is also hard to observe any spin-singlet structure in the *pp* elastic differential cross section below 2.8 GeV, since the spin-singlet resonances will be diluted by a large dominant spin-triplet "background".

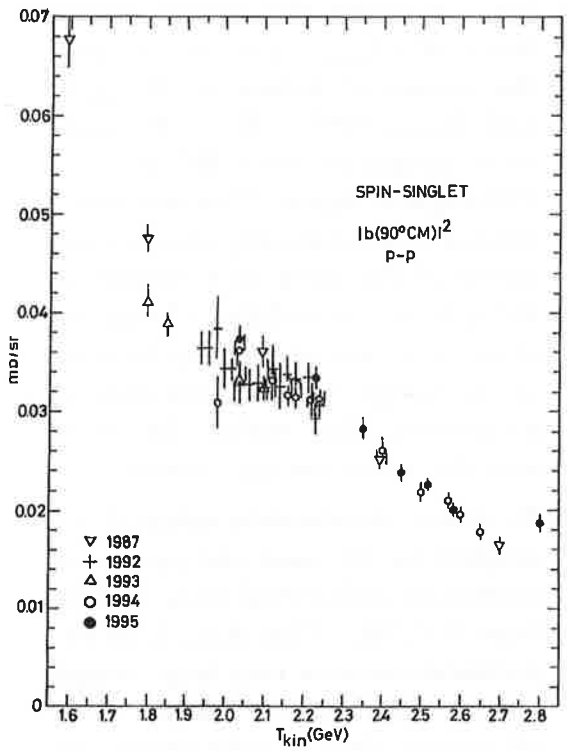

Fig. 10

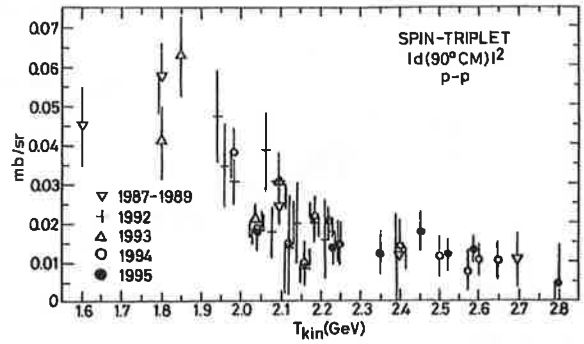

Fig. 11

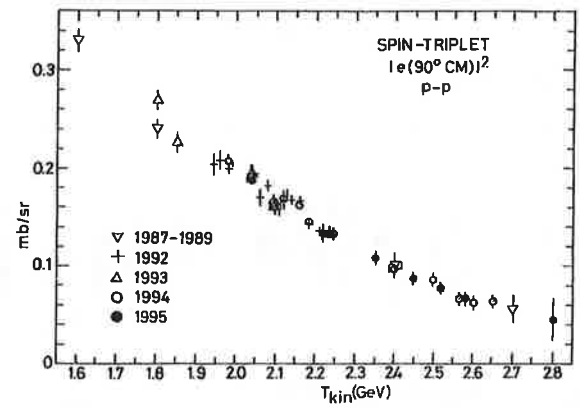

Fig. 12

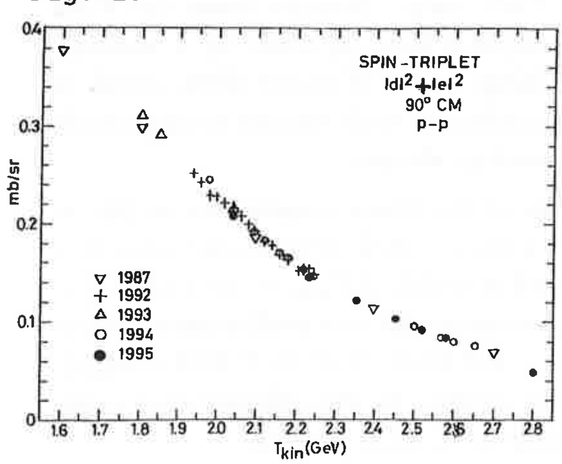

Fig. 13

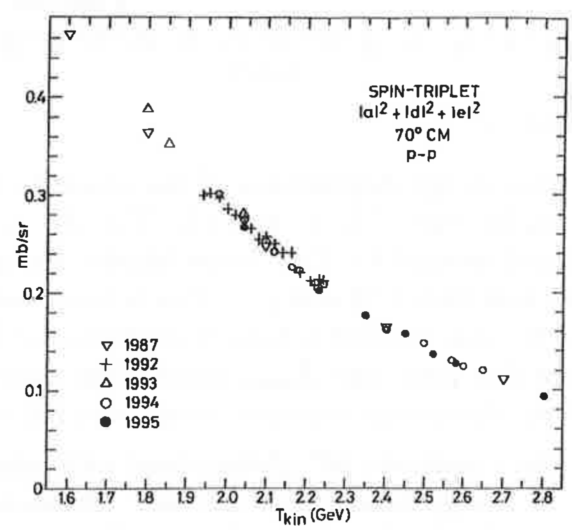

Fig. 14

The energy dependence of the spin-singlet amplitude $|b|^2$ provides only a "necessary" condition for the resonance. Note that an amplitude analysis cannot determine in which partial wave the resonances occur. An energy-dependent phase shift analysis using all the SATURNE II data measured at well-known energies in a large energy range would be required for this purpose. On the other hand, the condition, based on the amplitude behaviour is considerably stronger than those, provided by a behaviour of angular and energy distributions of unpolarized particle interaction.

The position of the singlet-spin resonance around $T_{kin} = 2.1$ GeV (mass 2.73 GeV) is consistent with the lowest lying exotic quark configurations in the isospin state I=1 as predicted by Lomon et al. using the Cloudy Bag Model and an R-matrix connection to long range meson exchange forces [16]. The position is also in qualitative agreement with Resonating Group Method calculations for constituent quark models (CQM), as predicted by Wong for the relativistic CQM, and by Kalashnikova, Narodetskii and Simonov for the non-relativistic CQM. The second singlet-spin resonance in $^1D_2$ was predicted with the mass of 80 MeV smaller than observed maximum for $|b|^2$.

Such dibaryons, when first proposed, were predicted to be at substantially lower energies using the MIT Bag Model, with an equilibrium radius that would be relevant if the multi-hadron system were confined and if there were no long range forces. For similar reasons, this lower range of predicted exotic masses was obtained by other early model calculations of exotic dibaryons.

Conclusion

The presented results considerably increase existing database and will allow an extension of the PSA towards high energies. They will improve the existing direct reconstruction of the scattering matrix up to 2.7 GeV. The analyzing power data are important for beam polarization measurements. Our results represent a consistent experimental indication for possible narrow resonances in spin-singlet *pp* elastic scattering. If the spin-singlet resonances suggested by our results are confirmed, its masses will be around 2.73 GeV and 2.96 GeV.

References

[1] R. Bernard et al., Nucl.Instrum.Methods **A249** (1986) 176
[2] J. Bystricky, C.Lechanoine-Leluc and F.Lehar, J.Phys. France **51** (1990) 2747
[3] R.A.Arndt, I.I. Strakovsky, and R.L.Workman Phys.Rev **C50** (1994) 2731, SAID program, solution FA95, The new PSA : R.A.Arndt, C.H. OH, I.I. Strakovsky, R.L. Workman, and F. Dohrman, will be published in Phys.Rev. C.
[4] C.D.Lac et al., J.Phys. France **51** (1990) 2689
[5] J.Ball et al., Nucl. Instrum. Methods **A381** (1996) 4
[6] D.Adams et al., Acta Polytechnica (Prague) **36** (1996) 11
[7] Ch. Allgower et al., Preprint LNS/Ph/97-01, Saclay 1997
[8] C. Lechanoine-Leluc and F.Lehar, Rev.Mod.Phys. **65** (1993) 47
[9] J.Bystricky, F.Lehar and P.Winternitz, J.Physique (Paris) **39** (1978) 1
[10] F.Lehar et al., Europhys.Lett. **3** (1987) 1175
[11] F.Perrot et al., Nucl.Phys. **B294** (1987) 1001
[12] J.Ball et al., Nucl.Instrum.Methods **A327** (1993) 308
[13] J.Arvieux et al., Preprint LNS/Ph/97-10, Saclay 1997
[14] F. Lehar et al., Nucl.Phys **B294** (1987) 1013
[15] Ch. Allgower et al., Preprint LNS/Ph/97-19, Saclay 1997
[16] E.L. Lomon, Colloque de Physique (France) **51** (1990) C6-363
[17] J. Yonnet et al., Nucl.Phys **A562** (1993) 362
[18] K.A.Jenkins et al., Phys.Rev. **D21** (1980) 2445
[19] J.Ball et al., Phys.Lett. **B320** (1994) 206